

MAY 31 1946

Continued  
P-36A/5

# NATIONAL ADVISORY COMMITTEE FOR AERONAUTICS

TECHNICAL NOTE

No. 1061

WIND-TUNNEL INVESTIGATION OF EFFECT OF WING LOCATION,  
POWER, AND FLAP DEFLECTION ON EFFECTIVE DIHEDRAL  
OF A TYPICAL SINGLE-ENGINE FIGHTER-AIRPLANE MODEL  
WITH TAIL REMOVED

By Warren A. Tucker

Langley Memorial Aeronautical Laboratory  
Langley Field, Va.



Washington  
May 1946

NACA LIBRARY  
LANGLEY MEMORIAL AERONAUTICAL  
LABORATORY  
Langley Field, Va.



3 1176 01433 3323

## NATIONAL ADVISORY COMMITTEE FOR AERONAUTICS

## TECHNICAL NOTE No. 1061

WIND-TUNNEL INVESTIGATION OF EFFECT OF WING LOCATION,  
POWER, AND FLAP DEFLECTION ON EFFECTIVE DIHEDRAL  
OF A TYPICAL SINGLE-ENGINE FIGHTER-AIRPLANE MODEL  
WITH TAIL REMOVED

By Warren A. Tucker

## SUMMARY

An investigation has been made of the effect of wing location, power, and flap deflection on the effective dihedral of a typical single-engine fighter-airplane model. The model, which was tested in the Langley 7- by 10-foot tunnel, had provisions for placing the wing in either one of two vertical locations. The wing was fitted alternatively with a full-span single slotted flap and with a full-span double slotted flap. The vertical and horizontal tails were removed for all tests.

The results are presented as curves of lateral-stability derivatives against lift coefficient. The observed effects are explained qualitatively. In addition to showing the usual loss in effective dihedral caused by changing from a high-wing to a low-wing design, the results indicated that this loss is increased by the application of power. The adverse effect of power increased with lift coefficient. The effect of flap deflection, which was unfavorable for all cases, appeared to be slightly greater for the low-wing model.

## INTRODUCTION

The problem of achieving sufficient effective dihedral for satisfactory handling qualities at low speeds and high thrust coefficients is becoming increasingly important, particularly with the advent of the high-powered low-wing fighter airplane. Some theoretical and

experimental work has been done on the effect of wing plan form and geometric dihedral on the effective dihedral of an isolated wing (references 1 and 2). Other experimental investigations of complete models of specific airplanes and of generalized models (references 3 to 7) have been made to determine the effect of wing plan form and wing location, and some theoretical work has been done on the effect of wing location (reference 8). There seems, however, to be little correlated information available regarding the mutual effects of power, flap deflection, and wing location.

A comprehensive investigation of the effects of wing location, power, and flap deflection on the static stability of a model of a single-engine fighter airplane is being conducted in the Langley 7- by 10-foot tunnel. The investigation includes longitudinal-stability and lateral-stability tests of the model as a high-wing and as a low-wing airplane. The tests have been made without flaps, with a full-span slotted flap having a chord 25 percent of the wing chord (0.25c), and with a 0.40c full-span double slotted flap. All tests have been made both with the propeller windmilling and with power on. Data on the effect of wing location, power, and flap deflection on effective dihedral with the tail removed have been obtained from the tests and are presented herein. Since the scope of the investigation was somewhat limited, particularly in the range of power, the conclusions are not very general.

#### APPARATUS AND MODEL

The tests were made in the Langley 7- by 10-foot tunnel, which is described in references 9 and 10. The basic model was a modified  $\frac{1}{5}$ -scale model of the Curtiss P-36A airplane (fig. 1). The vertical and horizontal tails were removed for all tests. The landing gear was retracted for all tests, since the aerodynamic effect of landing gears on stability is usually small.

The wing without flaps corresponded to the P-36A wing. The quarter-chord line of the wing was swept forward  $2.6^\circ$ . The 0.40c double slotted flap, which covered 93 percent span, was designed by use of the data of reference 11. The front part of the flap was deflected  $30^\circ$  with

respect to the flap-retracted position; the rear part of the flap was deflected  $30^\circ$  with respect to the front part. The rear part was used as a 0.25c single slotted flap by keeping the two parts of the flap in the same position relative to each other but moving the whole flap so that the front part was in the retracted position. The front part of the flap was then faired to the airfoil contour with modeling clay for tests of the wing with a single slotted flap. The details of the flap are shown in figure 2.

The model had a three-blade right-hand metal propeller. The propeller was driven by a 56-horsepower water-cooled induction motor mounted in the fuselage nose. The motor speed was measured by use of a cathode-ray oscillograph, which indicated the output of a small alternator connected to the shaft of the motor. The time base for the oscillograph pattern was controlled by an audio oscillator of the electrically driven tuning-fork type, the frequency of which was known within  $\pm 0.1$  percent. The propeller blade angle was set at  $25^\circ$  at the 0.75-radius station for all the tests. The side-force factor of the propeller (see reference 12) was 70.2.

## TESTS AND RESULTS

Test conditions.- All tests, except the power-on tests of the model with the double slotted flap, were made at a dynamic pressure of 16.37 pounds per square foot, which corresponds to a velocity of 80 miles per hour at standard sea-level conditions. In order to obtain the required thrust coefficients from the model motor, the power-on tests of the model with the double slotted flap were made at a dynamic pressure of 12.53 pounds per square foot, which corresponds to a velocity of 70 miles per hour at standard sea-level conditions. The corresponding test Reynolds numbers for these velocities were about 1,000,000 and 875,000, respectively, based on the model wing mean aerodynamic chord of 16.32 inches. The corresponding effective Reynolds numbers, based on the tunnel turbulence factor of 1.6, were about 1,600,000 and 1,400,000, respectively.

Coefficients and symbols.- The results of the tests are presented in the form of standard NACA nondimensional coefficients of forces and moments. Rolling-moment and

yawing-moment coefficients are given about the center-of-gravity location shown in figure 1 (26.7 percent M.A.C.). The data are referred to a system of axes in which the Z-axis is in the plane of symmetry and perpendicular to the relative wind, the X-axis is in the plane of symmetry and perpendicular to the Z-axis, and the Y-axis is perpendicular to the plane of symmetry. The axis system is shown in figure 3.

The coefficients and symbols used herein are defined as follows:

$C_L$	lift coefficient ( $Z/qS$ )
$C_{D_R}$	resultant-drag coefficient ( $X/qS$ )
$C_Y$	lateral-force coefficient ( $Y/qS$ )
$C_L$	rolling-moment coefficient ( $L/qSb$ )
$C_m$	pitching-moment coefficient ( $M/qS\bar{c}$ )
$C_n$	yawing-moment coefficient ( $N/qSb$ )
$T_c'$	effective thrust coefficient based on wing area ( $T_e/qS$ )
$T_c$	effective thrust coefficient based on propeller disk area ( $T_e/\rho V^2 D^2$ )

where

Z	lift
X	resultant drag
Y	lateral force
L	rolling moment
M	pitching moment
N	yawing moment
$T_e$	effective thrust, pounds
q	dynamic pressure, pounds per square foot ( $\frac{1}{2}\rho V^2$ )

- D model propeller diameter (2.0 ft)
- S model wing area (9.44 sq ft)
- b model wing span (7.45 ft)
- c model wing chord
- $\bar{c}$  model wing mean aerodynamic chord (16.32 in.)
- and
- $\rho$  mass density of air, slugs per cubic foot
- V velocity, feet per second
- R propeller radius
- n propeller speed, revolutions per second
- $\beta$  model propeller blade angle at 0.75R
- $\eta$  propeller efficiency
- $\alpha_T$  angle of attack of thrust line, degrees
- $\psi$  angle of yaw, degrees
- $\delta_f$  or  $\delta_{f2}$  deflection of rear part of flap with respect to front part, degrees
- $\delta_{f1}$  deflection of front part of flap with respect to flap-retracted position, degrees

The subscript  $\psi$  denotes the partial derivative of a coefficient with respect to the angle of yaw; for example,

$$C_{l\psi} = \frac{\partial C_l}{\partial \psi}$$

Test procedure.— Propeller calibrations were made by measuring the resultant drag of the model at zero angle of attack, with flaps neutral, and with tail removed for a range of propeller speed. The effective thrust coefficient based on wing area was then computed from the relation

$$T_c' = C_D - C_{DR}$$

where  $C_D$  is the drag coefficient of the model with the propeller removed. Motor torque, from which the propeller efficiency was computed, was measured with a built-in strain-gage torque dynamometer. The propeller calibration, which was made for only the low-wing model, is shown in figure 4; it is thought that the calibration for the high-wing model would be the same.

The variations of the effective thrust coefficient based on wing area  $T_c'$  and the effective thrust coefficient based on propeller disk area  $T_c$  with the lift coefficient  $C_L$  used for the tests are given in figure 5. A straight-line variation was used because this variation is a close approximation to the variation for airplanes with constant-speed propellers operating at constant power. The use of a straight-line variation is an assumption that  $\eta/\sqrt{C_L}$  is a constant; for this case, the value of  $\eta/\sqrt{C_L}$  was about 0.98. Although this assumption requires propeller efficiencies that would never be reached at low lift coefficients on an actual airplane, the error in  $T_c'$  is small because the values of  $T_c'$  are small. The approximate amount of airplane engine horsepower represented is given in figure 6 for various assumed wing loadings and model scales. The horsepower represented is proportional to the wing loading raised to the three-halves power and to the reciprocal of the square of the model scale.

Tests were made through the range of angle of attack and at angles of yaw of  $5^\circ$  and  $-5^\circ$  to determine the slopes  $C_{L\psi}$ ,  $C_{N\psi}$ , and  $C_{Y\psi}$  for various power conditions and model configurations. A linear variation between  $\psi = -5^\circ$  and  $\psi = 5^\circ$  was assumed for the corresponding coefficients  $C_L$ ,  $C_N$ , and  $C_Y$ . The results therefore are not necessarily applicable at large angles of yaw.

Corrections.- All data for power-on tests have been corrected for tares caused by the model support strut. The data for windmilling tests have not been corrected for these tares because of the limited time available for the tests; it is believed that the tares for the windmilling condition would be relatively small.

The angles of attack and the drag coefficients have been corrected for tunnel-wall effects. The corrections were computed as follows:

$$\Delta\alpha_T = 57.3\delta_w \frac{S}{C} C_L \quad (\text{deg})$$

$$\Delta C_D = \delta_w \frac{S}{C} C_L^2$$

where

$\delta_w$  jet-boundary correction factor at wing (0.113)

$S$  model wing area (9.44 sq ft)

$C$  tunnel cross-sectional area (69.59 sq ft)

The corrections were added to the test data.

Results.- The parameters  $C_{L\psi}$ ,  $C_{n\psi}$ , and  $C_{Y\psi}$  obtained at angles of yaw of  $\pm 5^\circ$  are given in figure 7. The curves of  $C_{n\psi}$  and  $C_{Y\psi}$  are included for completeness in these standard lateral-stability plots. Figures 8, 9, and 10, showing the effects on  $C_{L\psi}$  of wing location, power, and flap deflection, respectively, were obtained by taking the increments between the appropriate curves of figure 7. Figure 11 shows the aerodynamic characteristics in pitch of the model at zero yaw. The effect of power on the lift coefficient, presented in figure 12, was obtained by taking the increment between the appropriate curves of figure 11.

## DISCUSSION

In the following discussion, the observed effects are noted and some attempt is made to explain them qualitatively. A quantitative explanation seems impossible at the present stage of knowledge, because of the absence of any adequate theory covering the complex flows involved.



Effect of wing location.- The low-wing model was tested with a geometric dihedral angle of  $6^\circ$ , measured to the chord plane. When the wing was shifted to the high location, an estimate was made from reference 3 of the amount the geometric dihedral angle would have to be decreased in order to give the same effective dihedral for the high-wing and the low-wing models with flaps retracted and propeller windmilling. The estimated necessary change in geometric dihedral angle

(about  $4\frac{1}{2}^\circ$ ) caused the upper surface of the wing in the high location to be very nearly straight; for ease of construction, therefore, the upper surface was actually made straight. The dihedral angle of the chord plane was then  $1.9^\circ$ . The curve of figure 8 for the model with propeller windmilling and flaps retracted shows that the aim of achieving no change in effective dihedral between the low-wing and the high-wing configurations was very nearly realized. The curve shows that the low-wing model has about  $1^\circ$  effective dihedral less than the high-wing model over most of the lift-coefficient range ( $1^\circ$  of effective dihedral corresponds to  $C_{L\psi} = 0.0002$ ). The effect of power with flaps retracted was to increase this difference in effective dihedral between the high-wing and low-wing configurations. The reason for this effect is discussed more fully in the section on the effect of power.

The decrease in effective dihedral caused by lowering the wing can be explained by considering the flow that occurs over and under the fuselage when the model is yawed. The type of flow is illustrated in figure 13. This transverse flow increases the angle of attack near the fuselage of the leading wing in the high location and decreases the angle of attack of the leading wing in the low location. These changes in angle of attack result in a favorable rolling moment for the high-wing model and an unfavorable rolling moment for the low-wing model. This explanation shows why, in general, a high-wing airplane will exhibit greater effective dihedral than a corresponding low-wing airplane. Similar reasoning has been used in reference 8 to obtain a quantitative check between theoretical and experimental results. The explanation has sometimes been advanced that, when the model is yawed, a region of increased pressure is built up on the upwind side of the fuselage and a region of decreased

pressure is built up on the downwind side. This difference in pressure has been thought to give a favorable dihedral effect if the wing is high or an unfavorable effect if the wing is low. This pressure difference occurs, however, only when the cross-sectional area of the fuselage is increasing with distance backward along the fuselage - near the nose, for example. (A smaller opposite pressure difference will occur near the tail.) Since for most airplanes the wing is located in a region where the cross-sectional fuselage area is not changing greatly with distance along the fuselage and since experimental results may be checked quantitatively by considering angle-of-attack changes, it would seem that this explanation is not usually applicable.

With power on, the adverse effect of lowering the wing appears to be increased for all flap positions (fig. 8). A particularly large power effect is observed for the model with the double slotted flap. It should be noted that the curve for the model with double slotted flaps and propeller windmilling is not consistent with the other curves. This curve was derived from figure 7(c), in which the curve for the low-wing model in the windmilling condition is thought to be unreliable, perhaps because of a partial stall.

The foregoing discussion of the effects of wing location can be summarized as follows:

(1) Changing the wing from the high to the low location results in a decrease in effective dihedral.

(2) The difference in effective dihedral for the high-wing and the low-wing models is increased by the application of power.

Effect of power.- The effect of power (fig. 9) seems to be adverse for most cases. The effect is greater for the low-wing than for the high-wing model, and this difference in effect seems to increase with lift coefficient. An exception is noted in the curves for the double slotted flap. These curves, however, were derived from figure 7(c), in which the curve for the low-wing model in the windmilling condition is thought to be unreliable.

A possible explanation of the greater adverse effect of power on the low-wing model is given here. The slipstream affects the dihedral effect in two ways:

(1) The increased dynamic pressure in the slipstream results in an increased lift over the part of the wing immersed in the slipstream. When the model is yawed, the center line of the slipstream tends to pass over the trailing wing. The center of pressure of the added lift due to the slipstream thus lies somewhere on the trailing wing. The resulting rolling moment is therefore unfavorable.

(2) The increased dynamic pressure over the fuselage intensifies the effect of wing-fuselage interference which, as has been seen, is in general favorable for the high-wing and unfavorable for the low-wing model.

If the magnitude of the first effect is assumed to be almost independent of the vertical location of the wing, or at least to be less sensitive to wing location than the magnitude of the second effect, it is apparent that power will have a smaller adverse effect on the high-wing than on the low-wing model. This difference in effect of power will increase with lift coefficient.

As has been mentioned, one effect of power on effective dihedral is an increase in the lift over the part of the wing covered by the slipstream, which results in an unfavorable spanwise shift of the center of pressure when the airplane is yawed. In order to show the increase caused by power, the increments of lift coefficient between the windmilling and power-on conditions at the same angle of attack have been obtained from figure 11 and plotted in figure 12. As was expected, the curves of figure 12 showed the same trends as those of figure 9. Again an exception is noted in the curve for the low wing with double slotted flap, which is unreliable.

The foregoing discussion of the effects of power are summarized as follows:

(1) The application of power results in a decrease in effective dihedral.

(2) The adverse effect of power is greater when the wing is in the low location than when the wing is in the high location.

(3) The adverse effect of power generally increases with lift coefficient.

Effect of flap deflection.- The model with the double slotted flap was not tested at a lift coefficient low enough to permit the determination of the effect of this flap on effective dihedral; the curves of figure 10 therefore show the effect of only the single slotted flap.

Flap deflection appears to be unfavorable for both wing locations and for both power conditions.

The effect of flap deflection seems to be of the same order of magnitude for both the power-on and the windmilling conditions, and there seems to be no regular variation with lift coefficient. Flap deflection seems to have a slightly greater adverse effect on the low-wing than on the high-wing model. Tail-on tests of the same model (unpublished data) showed that the adverse effect of flap deflection was slightly greater for the high-wing than for the low-wing model.

The adverse effect of flap deflection on the effective dihedral of a swept-forward wing can be explained by considering separately the effect of yaw on the lift of each half of the wing. A swept-forward wing without flaps and with no dihedral is considered first. When the model is yawed, the trailing wing has a greater component of velocity normal to the quarter-chord line than the forward wing and thus has a greater lift. This difference in lift between the leading and the trailing wings results in an unfavorable rolling moment. By extending this reasoning to cover a range of angles of yaw, the slope of the curve of rolling-moment coefficient against angle of yaw is seen to be negative (negative effective dihedral). The opposite will be true, of course, for a swept-back wing. A more detailed analysis is given in reference 1. A wing with the flaps deflected is now considered. An analysis similar to the foregoing one can be applied to the additional lift caused by the flaps. In this case the velocities considered should be those normal to the hinge lines of the flaps. The analysis indicates that, if the flap hinge lines are swept forward (as on the

P-36A airplane), the flaps will give a negative increment of effective dihedral, regardless of wing sweep. This effect is illustrated in figure 10.

Since the increment in lift produced by deflecting the flaps can be considered constant throughout the range of lift coefficient, the increment in effective dihedral caused by flap deflection should also be constant. Although such is not quite the case in figure 10, there is no decided trend of the curves so that this reasoning seems to be valid and the variations of the curves from horizontal straight lines may be considered to be caused by other effects.

The foregoing discussion of the effects of deflecting the single slotted flap  $30^\circ$  is summarized as follows:

(1) The effect of flap deflection on effective dihedral is unfavorable for both wing locations and for both power conditions.

(2) This effect appears to be of the same order of magnitude for both the power-on and the windmilling conditions, for the limited range of thrust coefficients and lift coefficients investigated.

(3) Flap deflection appears to have a slightly greater adverse effect on the low-wing than on the high-wing model. Tail-on tests of the same model have showed a small opposite effect.

(4) There seems to be no definite variation of the effect of flap deflection with lift coefficient.

### CONCLUSIONS

From tests in the Langley 7- by 10-foot tunnel of a modified  $\frac{1}{5}$ -scale model of the Curtiss P-36A airplane with the quarter-chord line of the wing swept forward  $2.6^\circ$  and the tail removed, the following conclusions were drawn regarding the effects of wing location, power, and flap deflection on effective dihedral:

Effect of wing location.-

(1) Changing the wing from the high to the low location resulted in a decrease in effective dihedral.

(2) The difference in effective dihedral for the high-wing and the low-wing models was greater for the power-on condition than for the windmilling condition.

Effect of power.-

(1) The application of power resulted in a decrease in effective dihedral.

(2) Power had a greater adverse effect for the low-wing than for the high-wing model.

(3) The adverse effect of power generally increased with lift coefficient.

Effect of flap deflection (full-span single slotted flap only; flap hinge lines swept forward).-

(1) The effect of flap deflection on effective dihedral was unfavorable for both wing locations and for both the power conditions.

(2) The effect of flap deflection appeared to be of the same order of magnitude for the power-on and the windmilling conditions, for the limited range of thrust coefficients and lift coefficients investigated.

(3) Flap deflection appeared to have a slightly greater adverse effect on the low-wing than on the high-wing model. Tail-on tests of the same model have showed a small opposite effect.

(4) There seemed to be no definite variation of the effect of flap deflection with lift coefficient. This fact seems to substantiate a rough qualitative analysis, which indicates that the effect of flap deflection should not vary with lift coefficient.

Langley Memorial Aeronautical Laboratory  
National Advisory Committee for Aeronautics  
Langley Field, Va., January 2, 1945

## REFERENCES

1. Betz, A.: Applied Airfoil Theory. Unsymmetrical and Non-Steady Types of Motion. Vol. IV of Aerodynamic Theory, div. J, ch. IV, secs. 1-4, W. F. Durand, ed., Julius Springer (Berlin), 1935.
2. Pearson, Henry A., and Jones, Robert T.: Theoretical Stability and Control Characteristics of Wings with Various Amounts of Taper and Twist. NACA Rep. No. 635, 1938.
3. House, Rufus O., and Wallace, Arthur R.: Wind-Tunnel Investigation of Effect of Interference on Lateral-Stability Characteristics of Four NACA 23012 Wings, an Elliptical and a Circular Fuselage, and Vertical Fins. NACA Rep. No. 705, 1941.
4. Bamber, M. J., and House, R. O.: Wind-Tunnel Investigation of Effect of Yaw on Lateral-Stability Characteristics. II - Rectangular N.A.C.A. 23012 Wing with a Circular Fuselage and a Fin. NACA TN No. 730, 1939.
5. Recant, Isidore G., and Wallace, Arthur R.: Wind-Tunnel Investigation of Effect of Yaw on Lateral-Stability Characteristics. III - Symmetrically Tapered Wing at Various Positions on Circular Fuselage with and without a Vertical Tail. NACA TN No. 825, 1941.
6. Recant, I. G., and Wallace, Arthur R.: Wind-Tunnel Investigation of Effect of Yaw on Lateral-Stability Characteristics. IV - Symmetrically Tapered Wing with a Circular Fuselage Having a Wedge-Shaped Rear and a Vertical Tail. NACA ARR, March 1942.
7. Wallace, Arthur R., and Turner, Thomas R.: Wind-Tunnel Investigation of Effect of Yaw on Lateral-Stability Characteristics. V - Symmetrically Tapered Wing with a Circular Fuselage Having a Horizontal and a Vertical Tail. NACA ARR No. 3F23, 1943.

WTR L-459

8. Multhopp, H.: Aerodynamics of the Fuselage. NACA TM No. 1036, 1942.
9. Harris, Thomas A.: The 7 by 10 Foot Wind Tunnel of the National Advisory Committee for Aeronautics. NACA Rep. No. 412, 1931.
10. Wenzinger, Carl J., and Harris, Thomas A.: Wind-Tunnel Investigation of an N.A.C.A. 23012 Airfoil with Various Arrangements of Slotted Flaps. NACA Rep. No. 604, 1939.
11. Harris, Thomas A., and Recant, Isidore G.: Wind-Tunnel Investigation of NACA 23012, 23021, and 23030 Airfoils Equipped with 40-Percent-Chord Double Slotted Flaps. NACA Rep. No. 723, 1941.
12. Ribner, Herbert S.: Proposal for a Propeller Side-Force Factor. NACA RB No. 3L02, 1943.



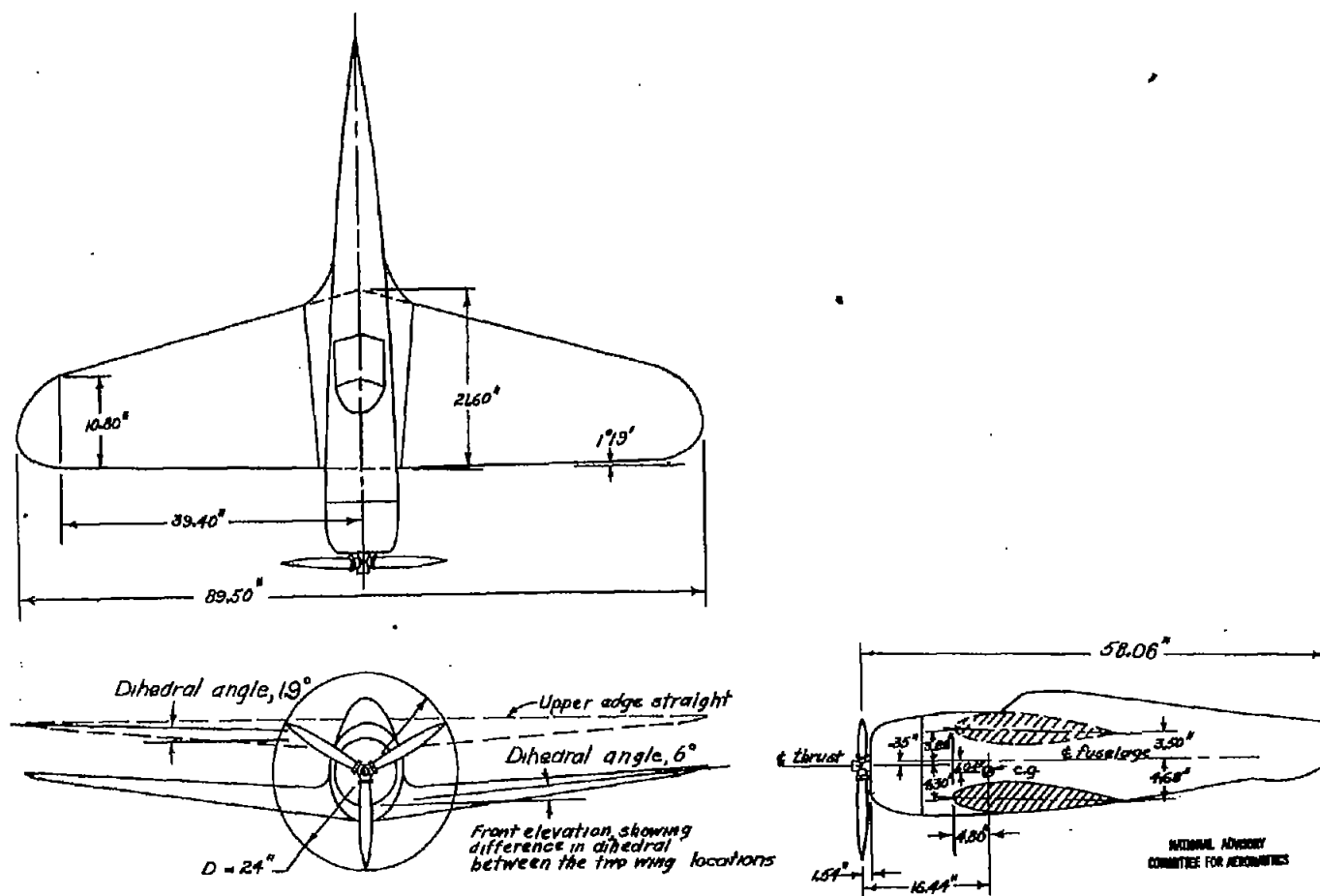


Figure 1. - Modified  $\frac{1}{5}$ -scale model of Curtiss P-36A airplane with tail removed. Neither single slotted nor double slotted flaps are shown. See figure 2 for flap details.

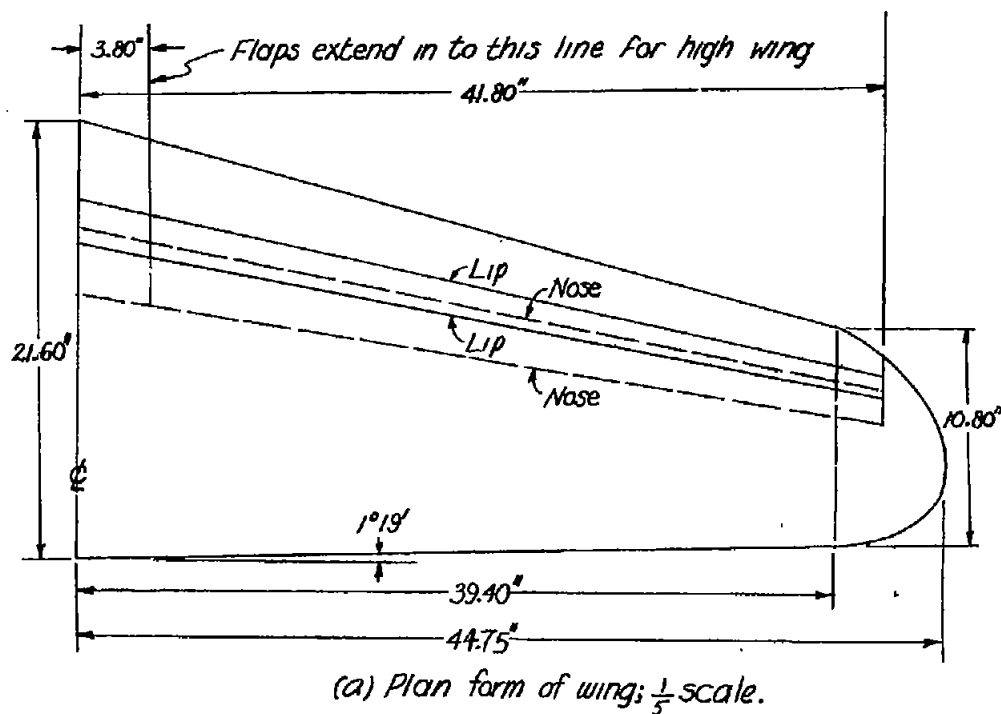
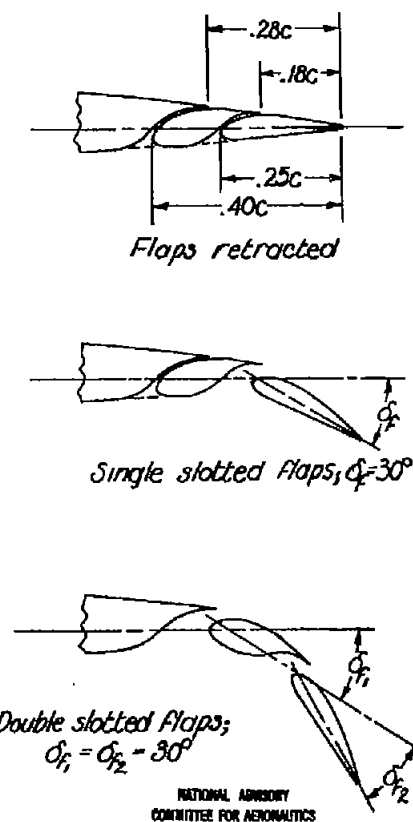
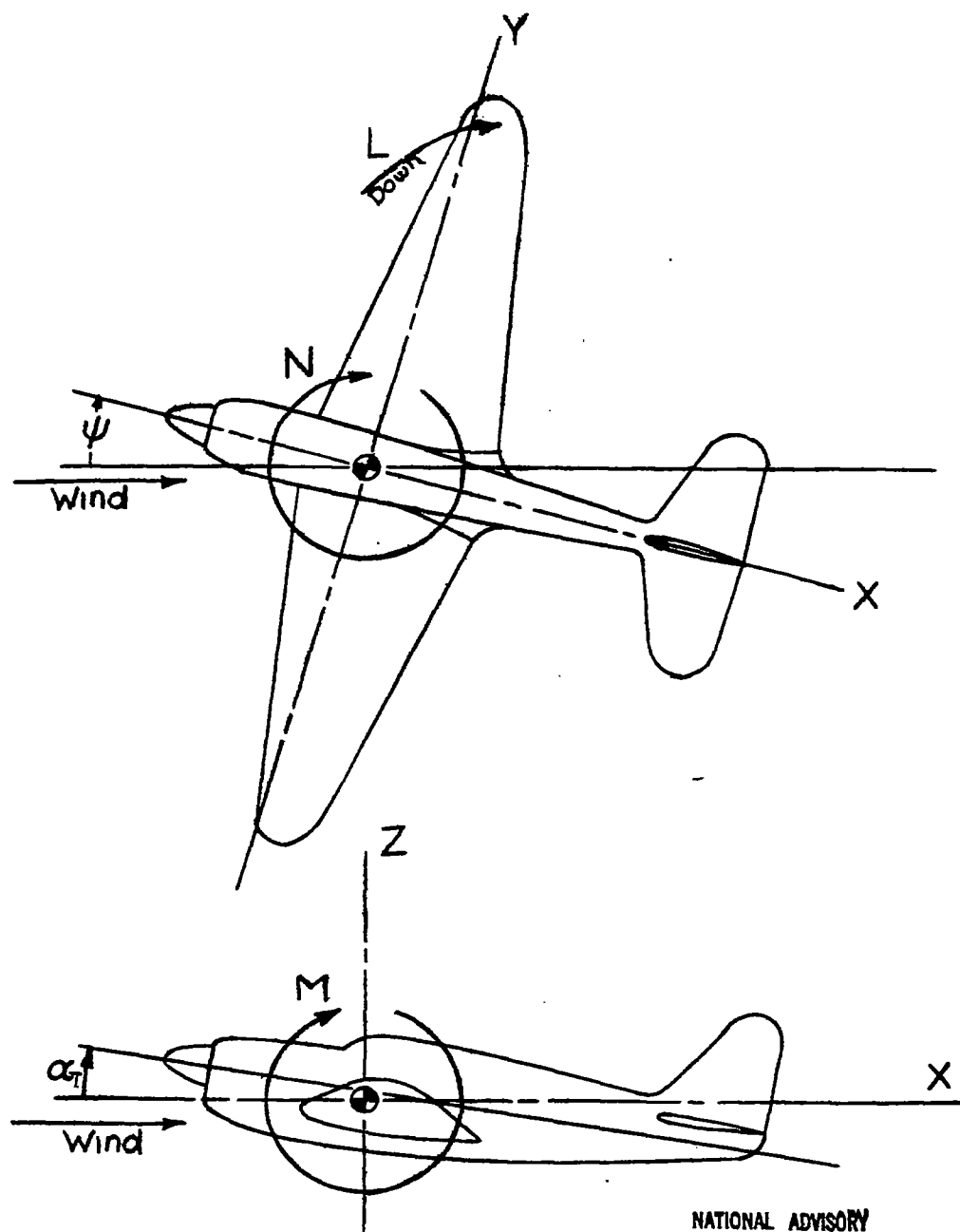


Figure 2.- Flap details of the modified  $\frac{1}{5}$ -scale model of the Curtiss P-36A airplane.





NATIONAL ADVISORY  
COMMITTEE FOR AERONAUTICS

Figure 3.- Notation of axis system used. Arrows indicate positive directions.

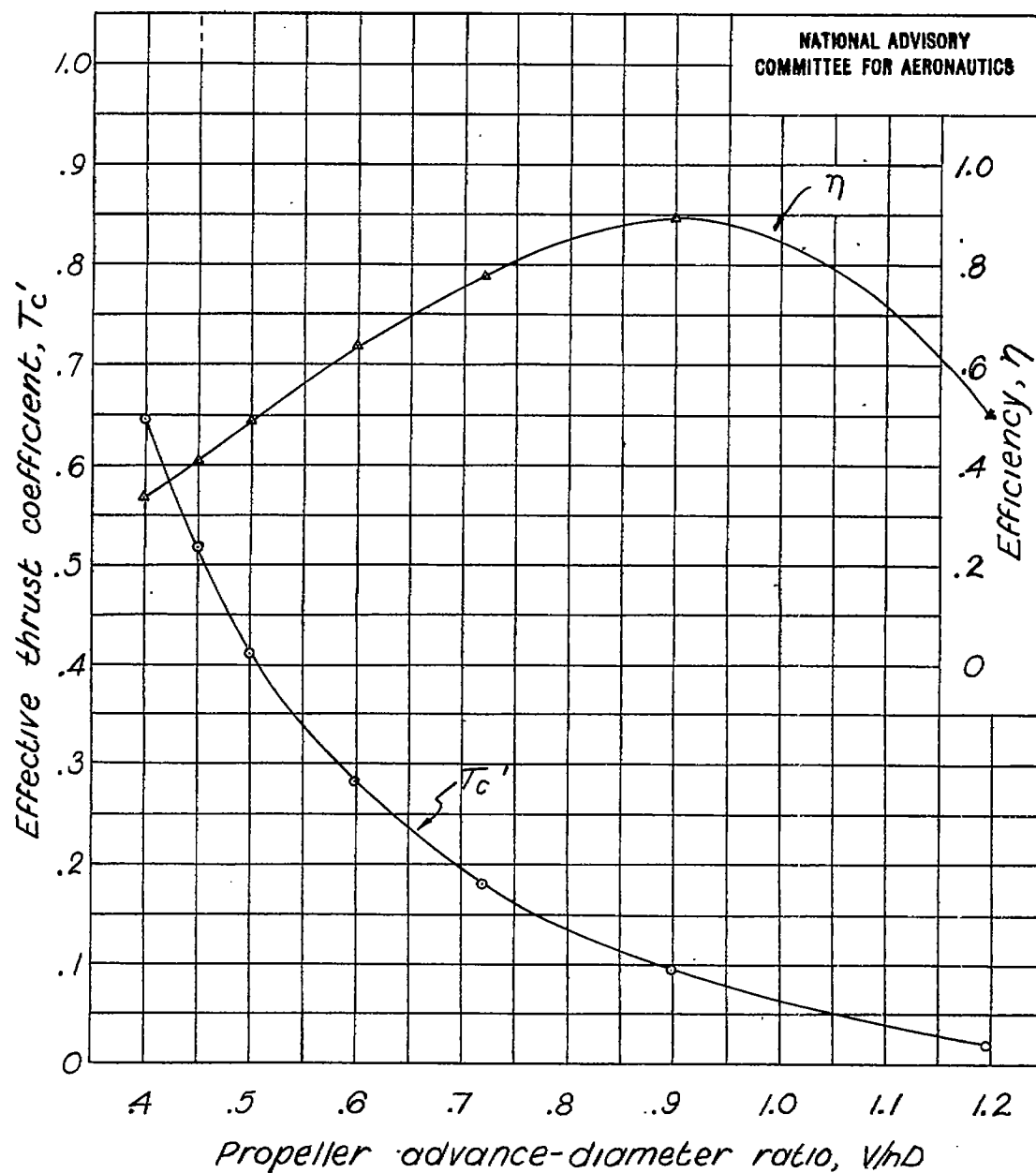


Figure 4.- Effective thrust coefficient and efficiency as functions of propeller advance-diameter ratio for the modified  $\frac{1}{2}$ -scale model of the Curtiss P-36A airplane.  $D=2.0$  feet;  $\beta=25^\circ$ .

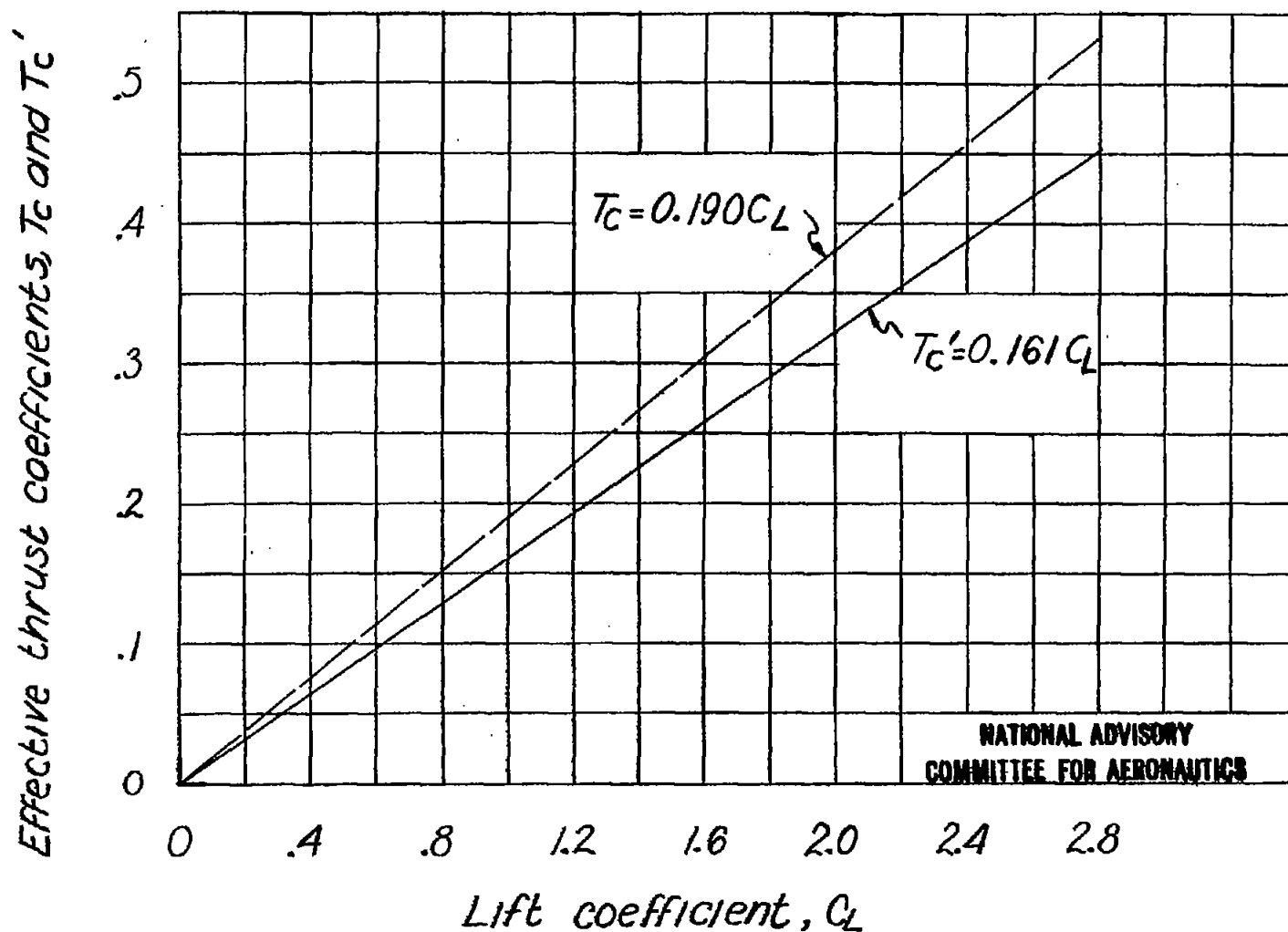


Figure 5.- Variation of effective thrust coefficients with lift coefficient.

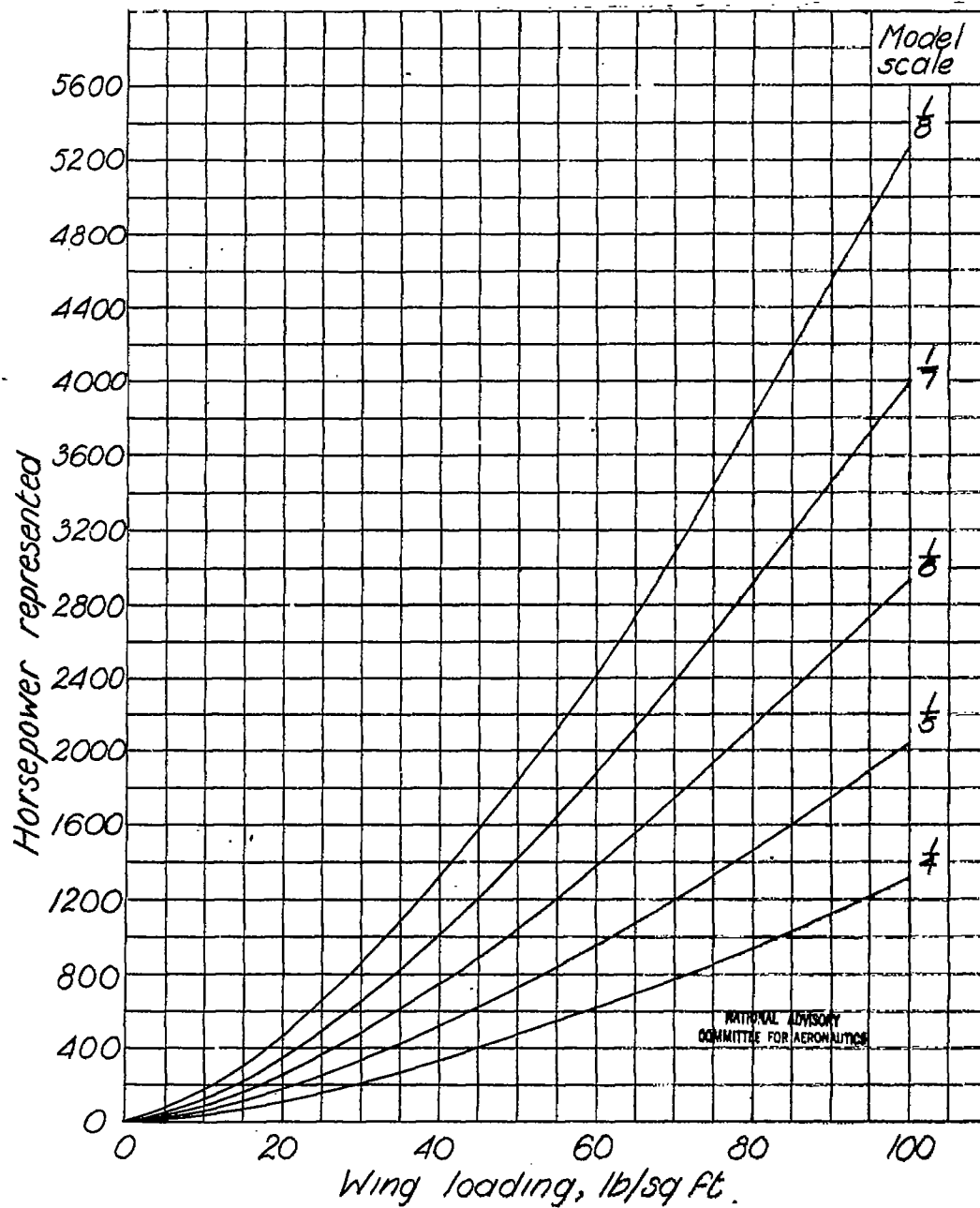
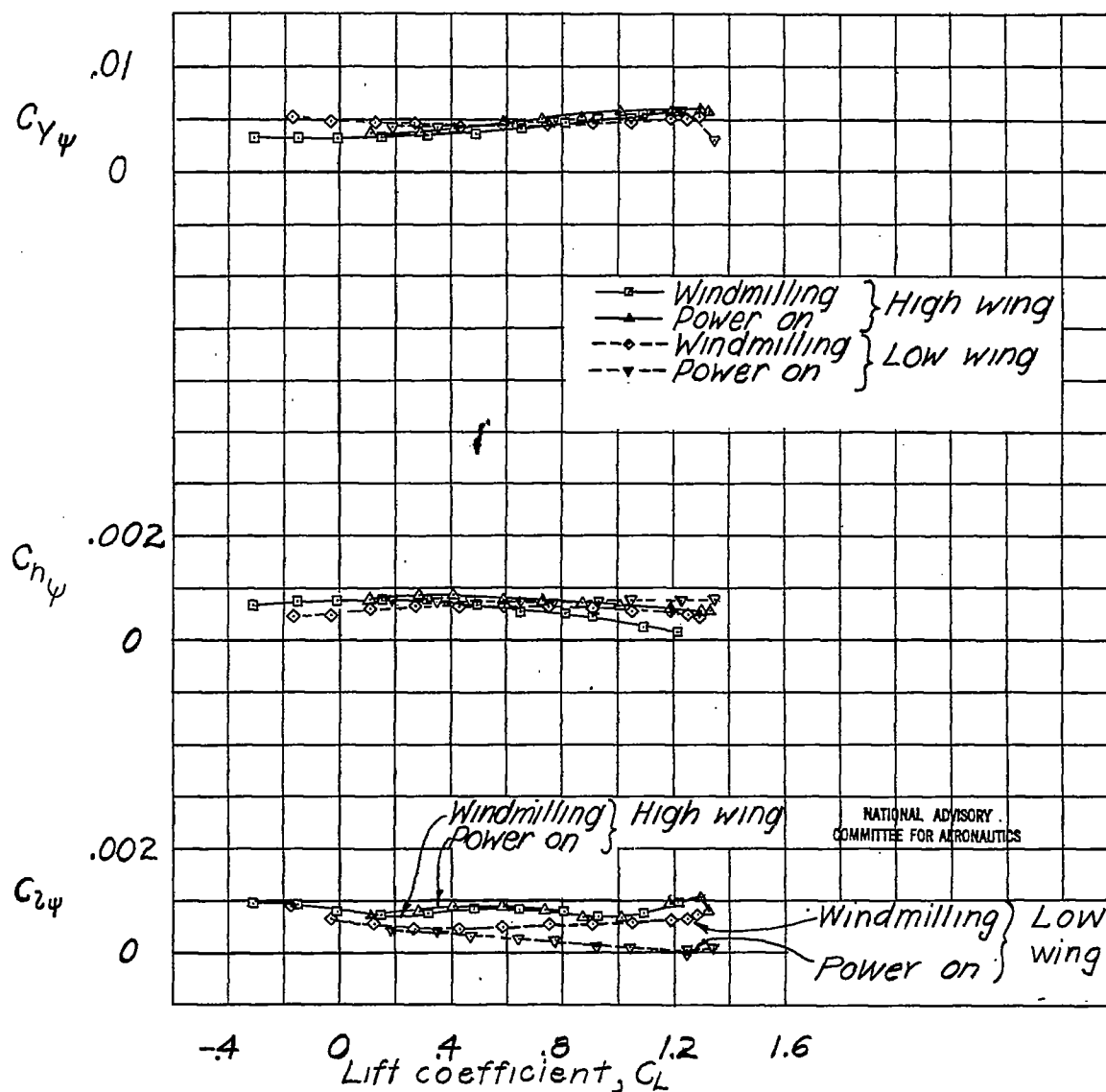
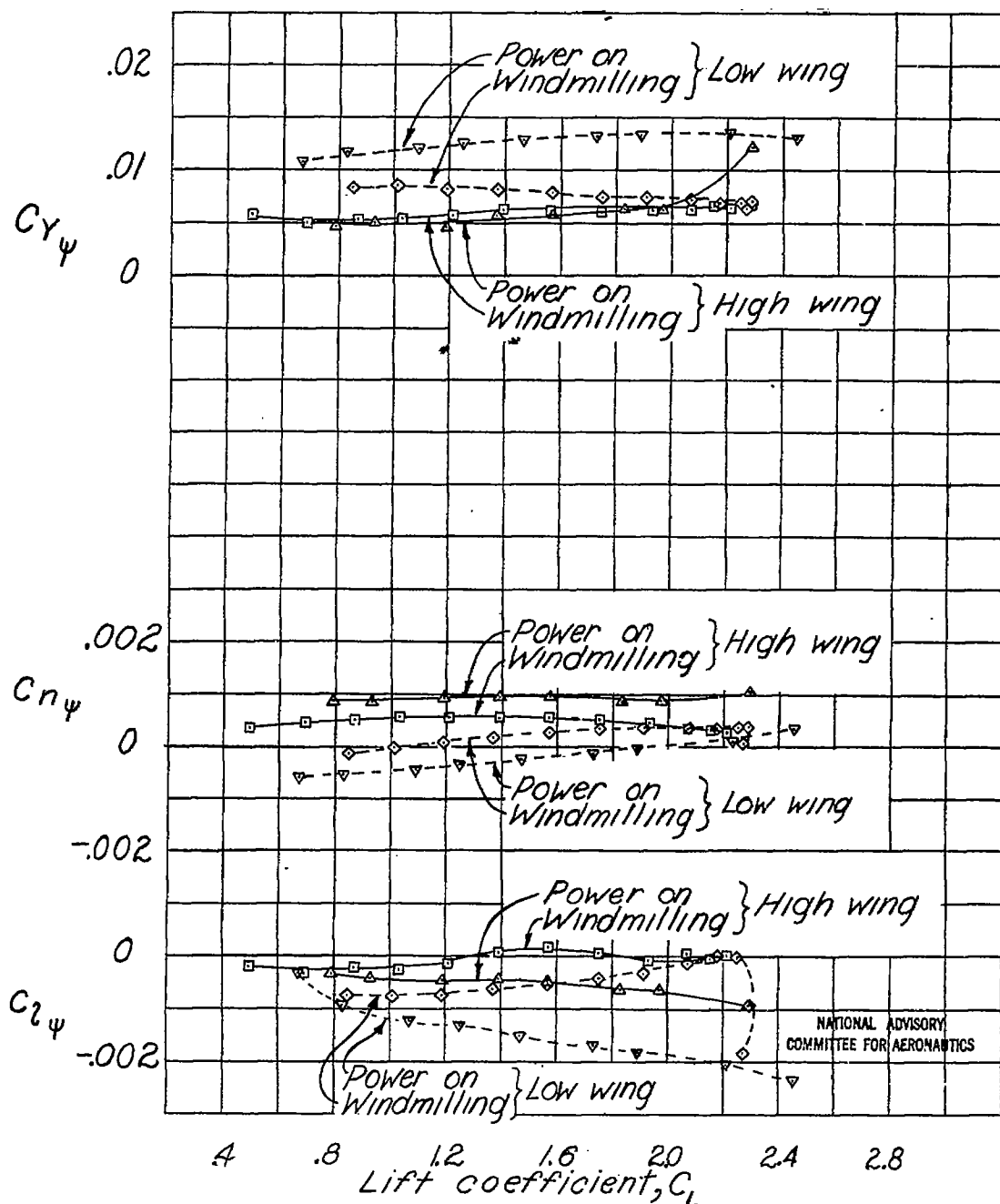


Figure 6.- Variation of approximate horsepower represented with airplane wing loading for various model scales.



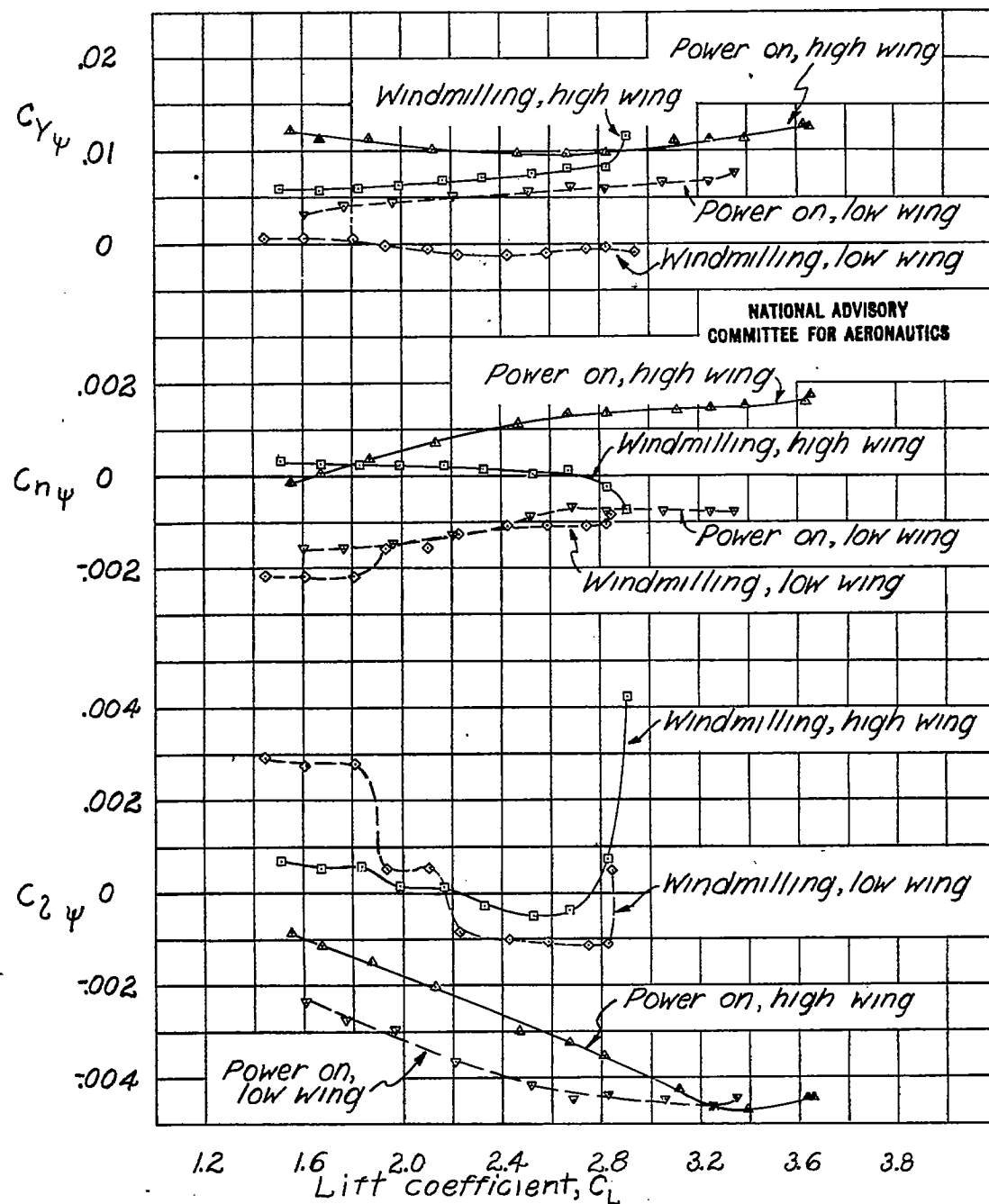
(a) Flaps retracted.

Figure 7.-Effect of wing location and power on the parameters  $C_{Y\psi}$ ,  $C_{N\psi}$ , and  $C_{L\psi}$ . Modified  $\frac{1}{2}$ -scale model of the Curtiss P-36A airplane; tail removed.



(b) Full-span single slotted flaps;  $\delta_f = 30^\circ$ .  
Figure 7.-Continued.





(c) Full-span double slotted flaps;  $\delta_{f_1} = \delta_{f_2} = 30^\circ$ .

Figure 7.-Concluded.

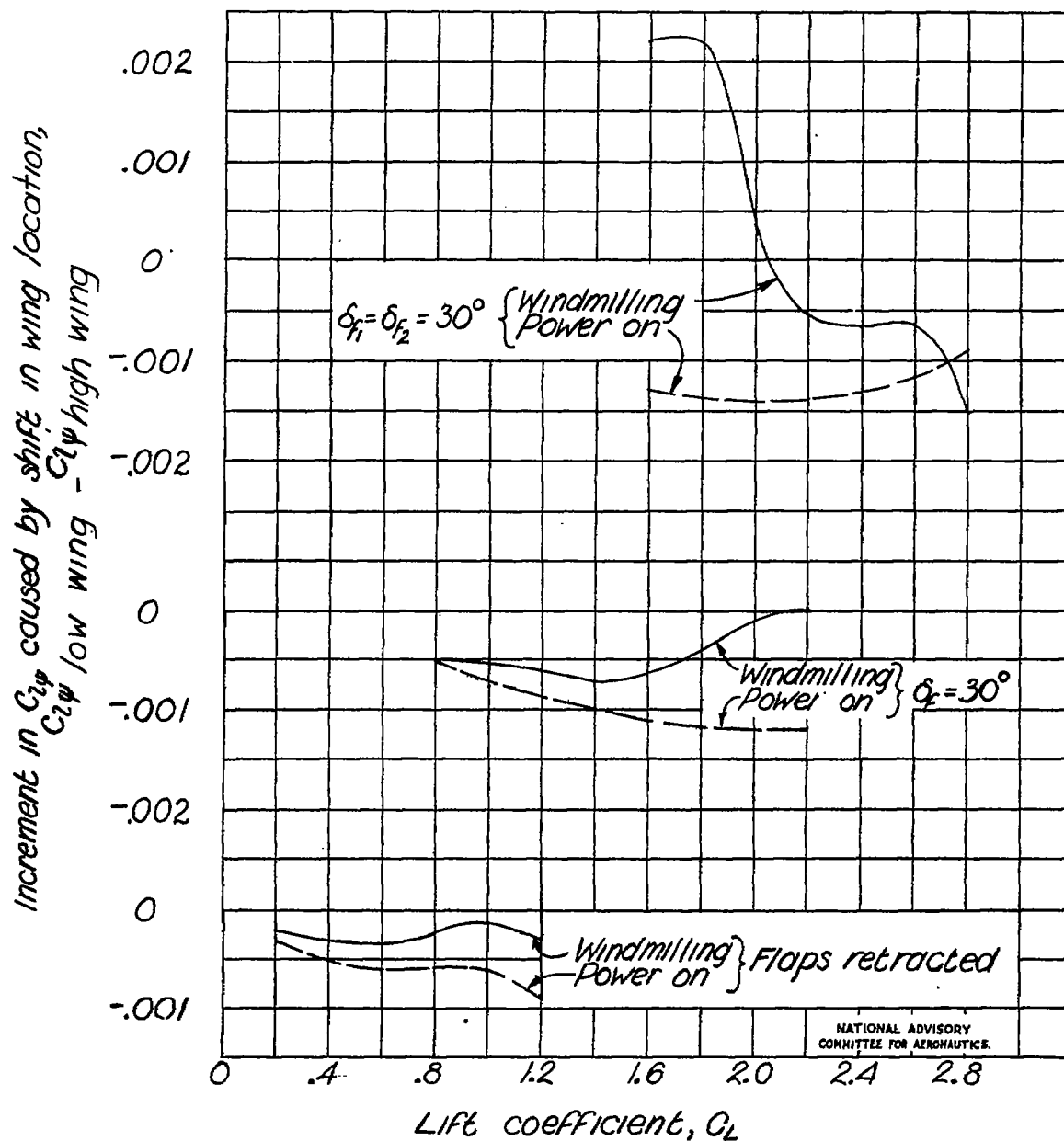


Figure 8.-Effect of wing location on  $C_{2\psi}$ . Modified  $\frac{1}{3}$ -scale model of the Curtiss P-36A airplane; tail removed.

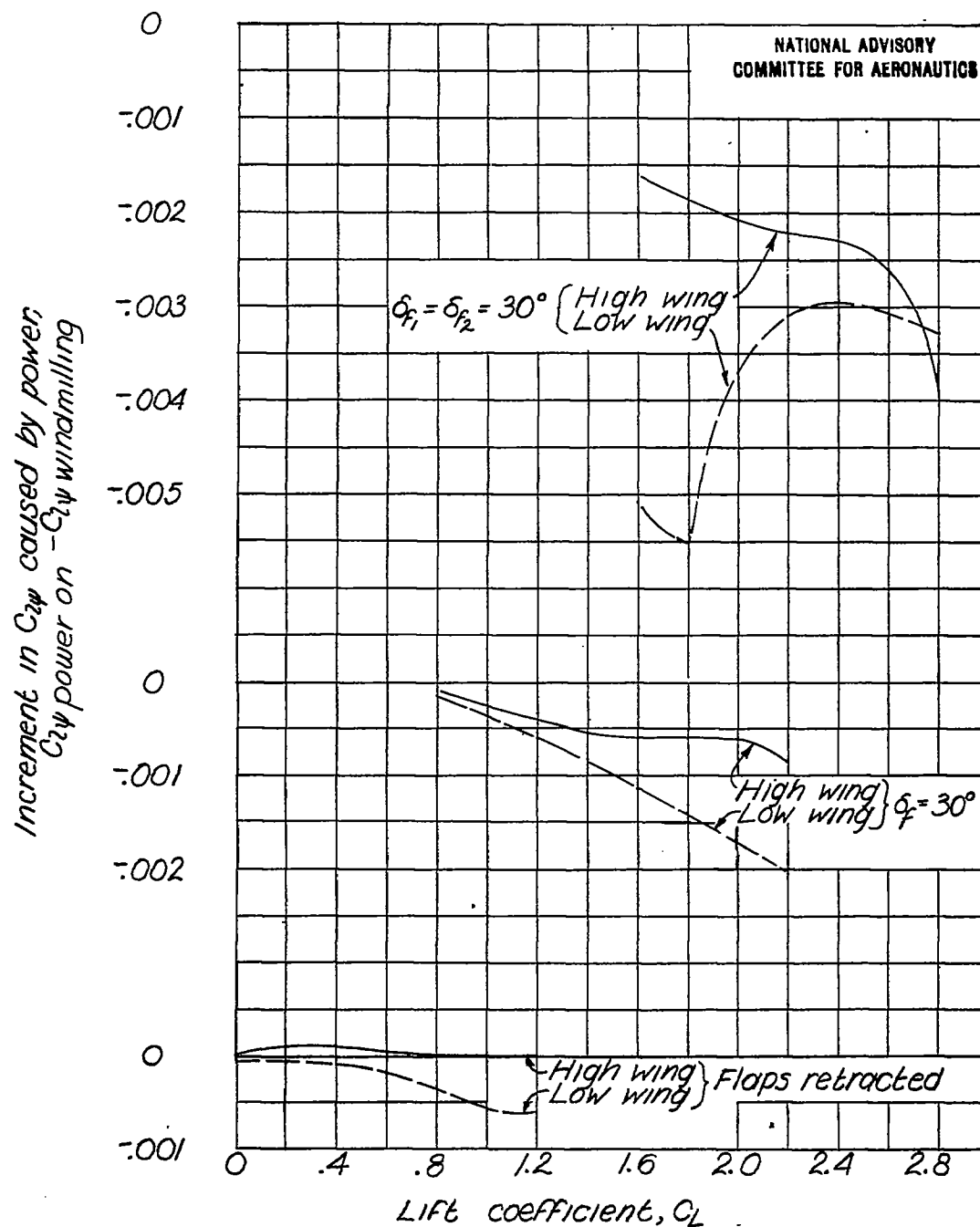


Figure 9.—Effect of power on  $C_{2\psi}$ . Modified  $\frac{1}{2}$ -scale model of the Curtiss P-36A airplane; tail removed.

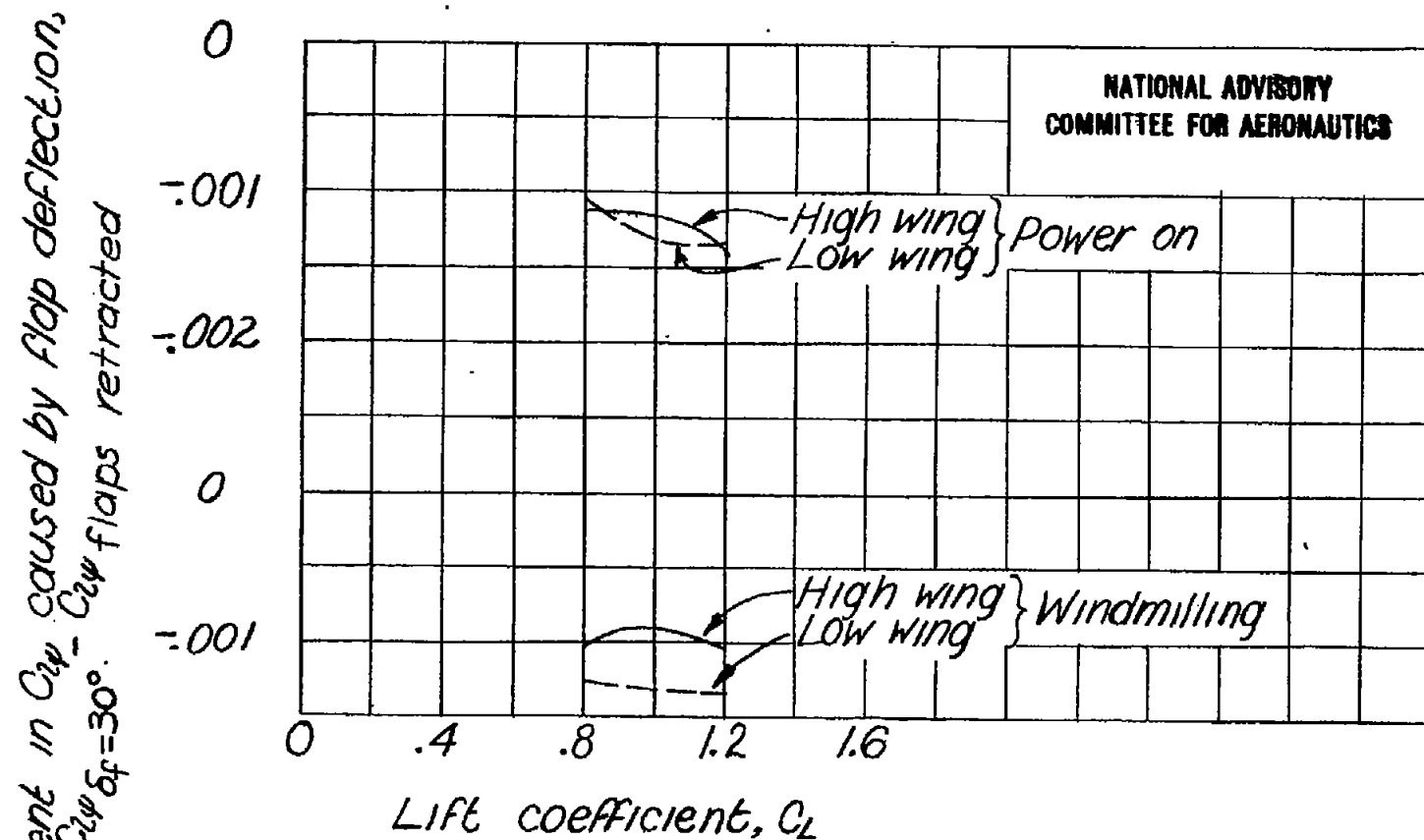
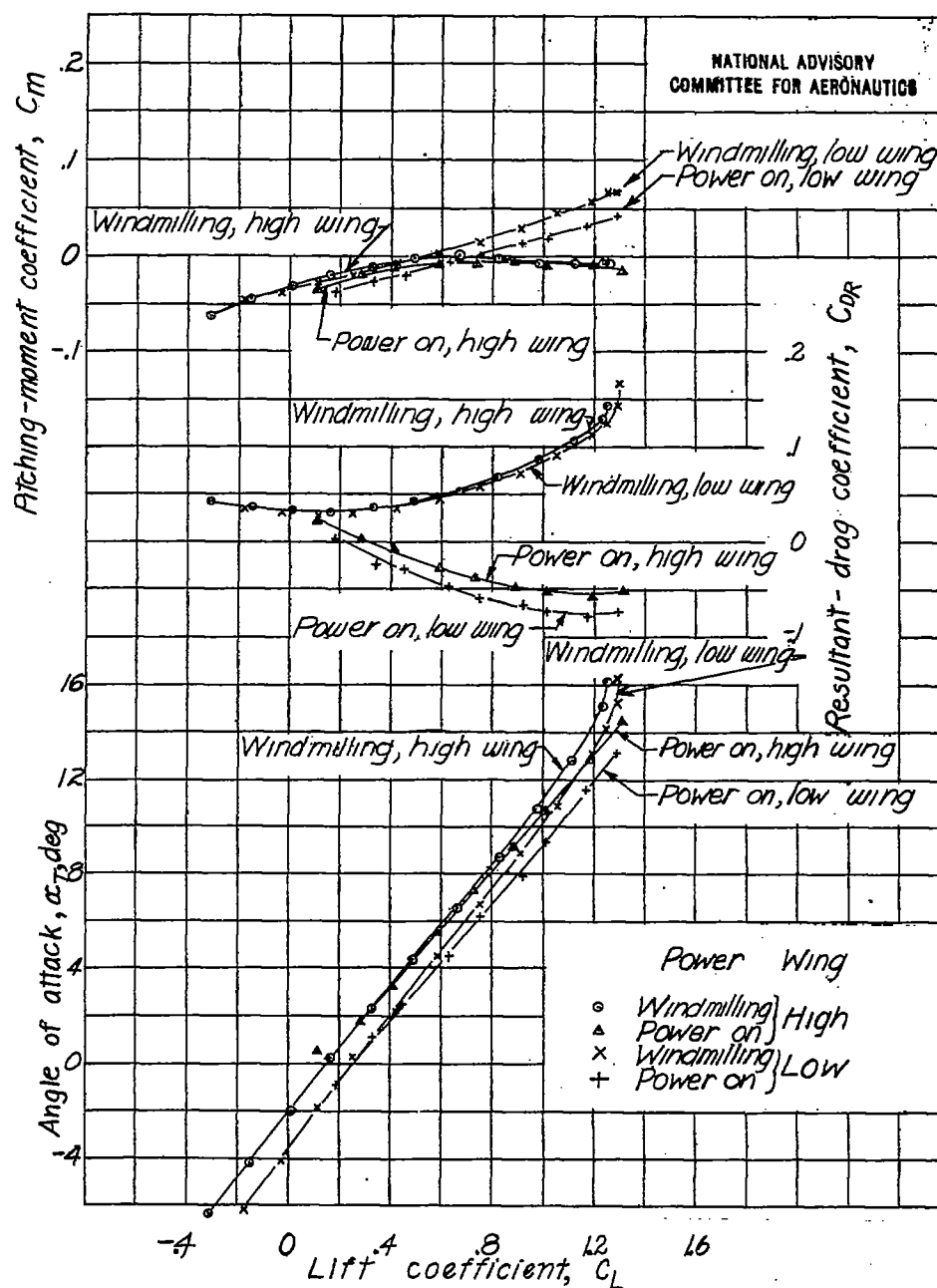
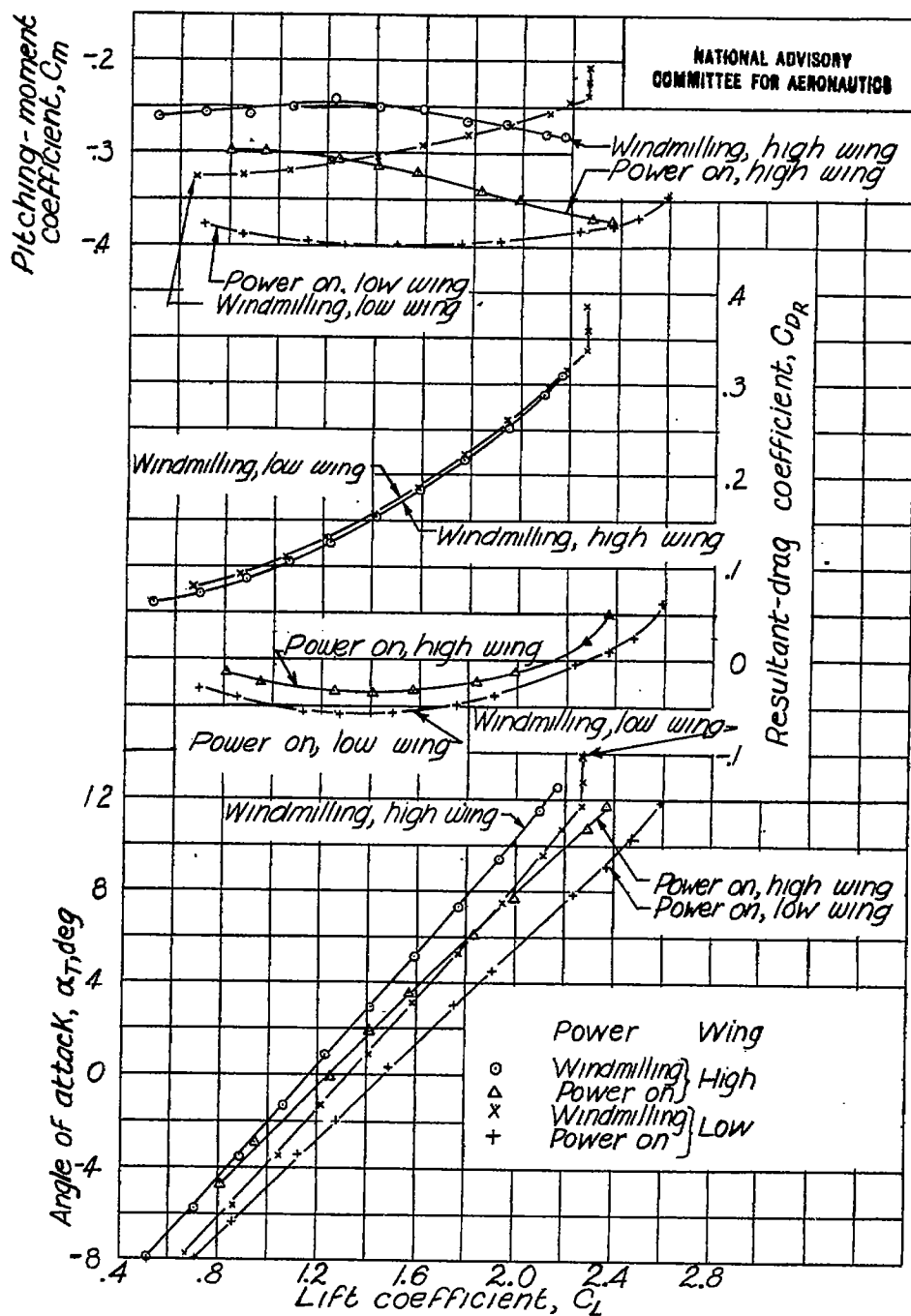


Figure 10.-Effect of flap deflection on  $C_{L\psi}$ . Modified  $\frac{1}{5}$ -scale model of the Curtiss P-36 A airplane; tail removed; full-span single slotted flap.



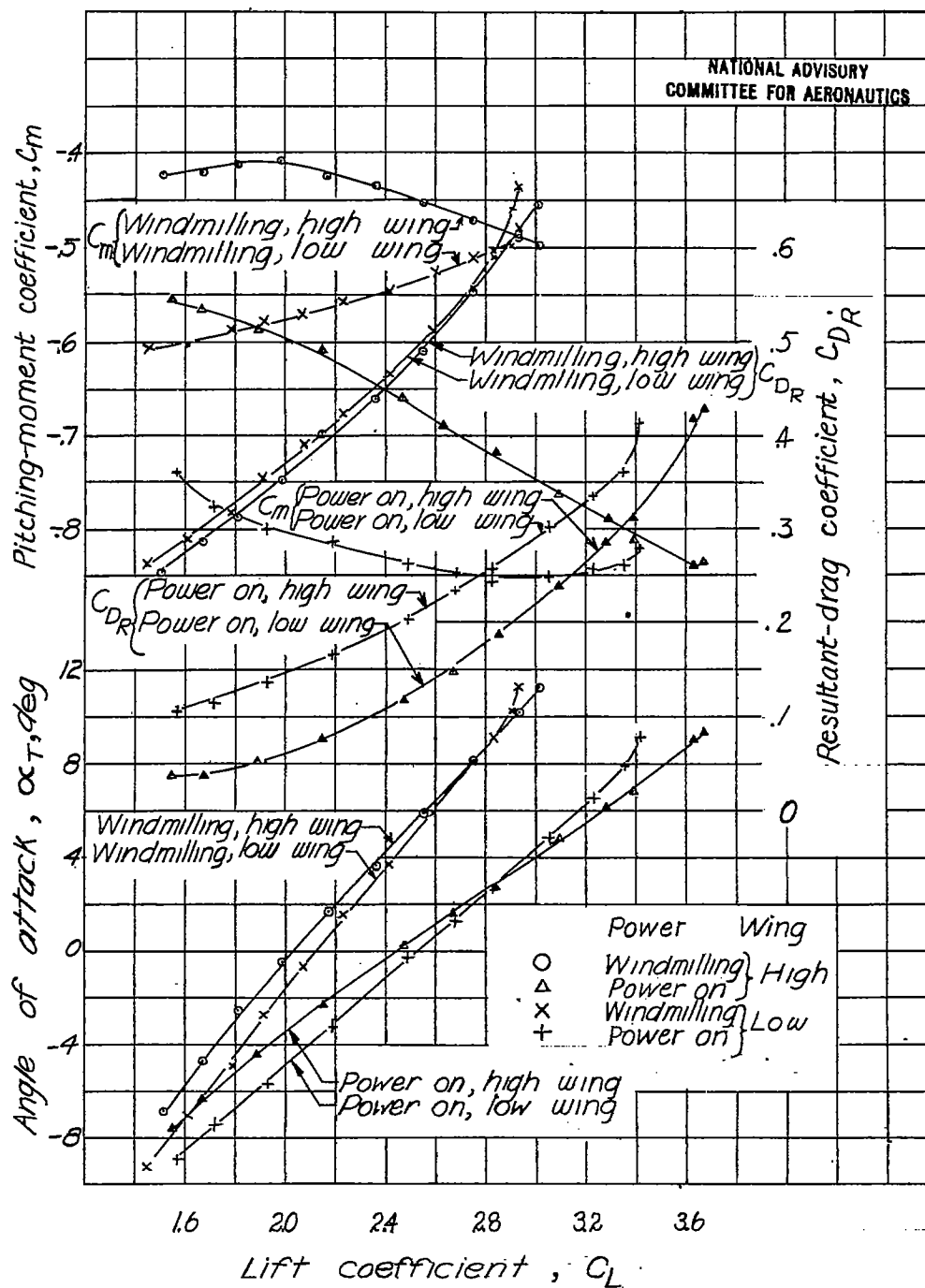
(a) Flaps retracted.

Figure 11.—Effect of wing location and power on the aerodynamic characteristics in pitch of a modified  $\frac{1}{2}$ -scale model of the Curtiss P-36A airplane; tail removed;  $\psi = 0^\circ$ .



(b) Full-span single slotted flaps;  $\delta_f = 30^\circ$ .

Figure 11.- Continued.



(c) Full-span double slotted Flaps;  $\delta_{F1} = \delta_{F2} = 30^\circ$ .

Figure 11.- Concluded.

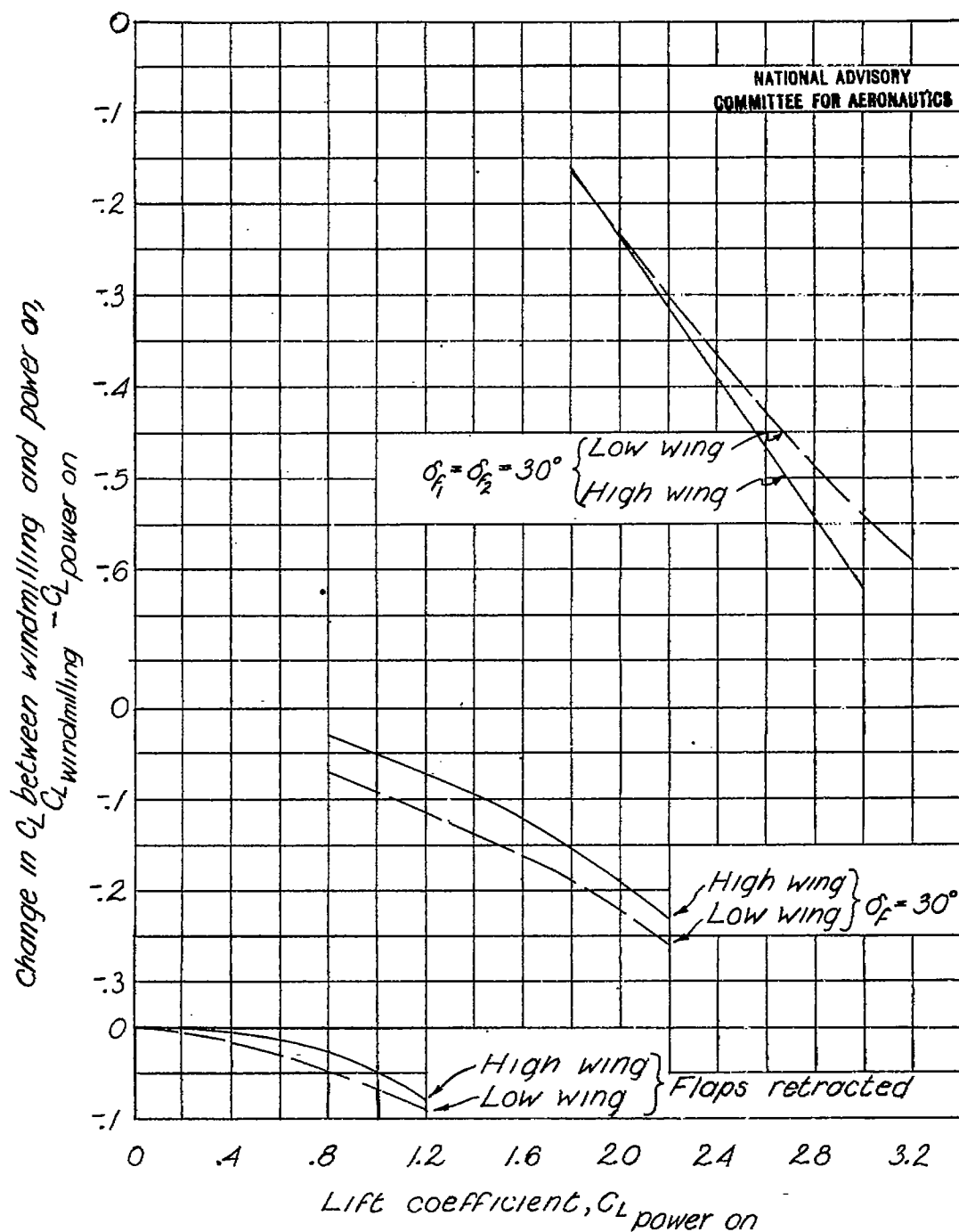
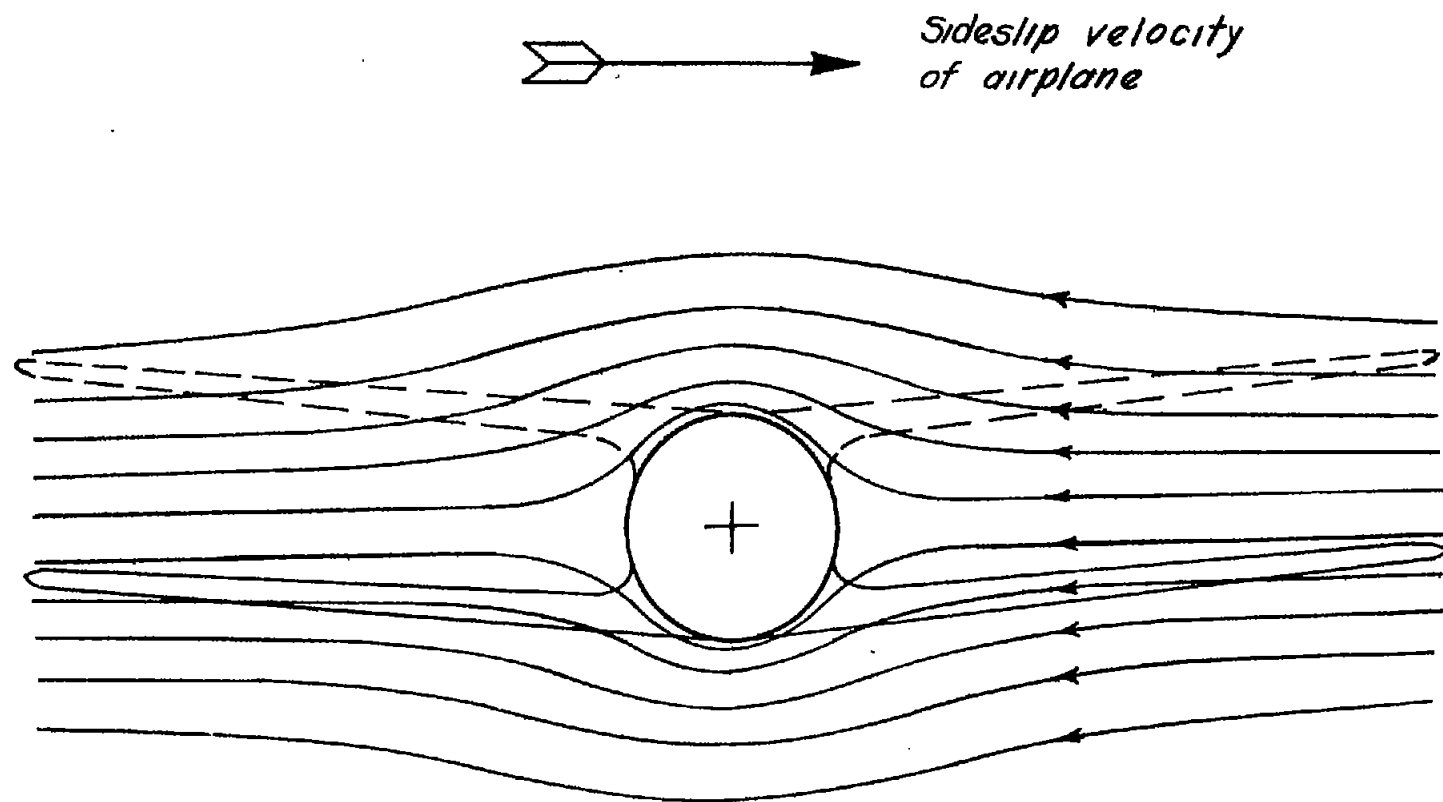


Figure 12.-Effect of power on lift coefficient.  
Modified  $\frac{1}{5}$ -scale model of the Curtiss P-36A  
airplane; tail removed.





NATIONAL ADVISORY  
COMMITTEE FOR AERONAUTICS

Figure 13.-Transverse flow caused by sideslip.